

Article

Modular Optic Force Sensor for a Surgical Device Using a Fabry–Perot Interferometer

Jumpei Arata ^{1,*}, Tatsuya Nitta ², Toshiki Nakatsuka ², Tomonori Kawabata ³, Tadao Matsunaga ⁴, Yoichi Haga ³, Kanako Harada ² and Mamoru Mitsuishi ²

¹ Department of Mechanical Engineering, Faculty of Engineering, Kyushu University, Fukuoka 8190395, Japan

² Department of Mechanical Engineering, School of Engineering, The University of Tokyo, Tokyo 1138656, Japan

³ Graduate School of Biomedical Engineering, Tohoku University, Sendai 9808579, Japan

⁴ Department of Electrical Engineering and Computer Science, Faculty of Engineering, Tottori University, Tottori 6808550, Japan

* Correspondence: jumpei@mech.kyushu-u.ac.jp

Received: 20 July 2019; Accepted: 14 August 2019; Published: 21 August 2019



Abstract: The ability to sense force in surgery is in high demand in many applications such as force feedback in surgical robots and remote palpation (e.g., tumor detection in endoscopic surgery). In addition, recording and analyzing surgical data is of substantial value in terms of evidence-based medicine. However, force sensing in surgery remains challenging because of the specific requirements of surgical instruments, namely, they must be small, bio-compatible, sterilizable, and tolerant to noise. In this study, we propose a modular optic force sensor using a Fabry–Perot interferometer that can be used on surgical devices. The the proposed sensor can be implemented like a strain gauge, which is widely used in industrial applications but not compatible with surgery. The proposed sensor includes two key elements, a fiber-optic pressure sensor using a Fabry–Perot interferometer that was previously developed by one of the authors and a structure that includes a carbide pin that contacts the pressure sensor along the long axis. These two elements are fixed in a guide channel fabricated in a $3 \times 2 \times 0.5$ mm sensor housing. The experimental results are promising, revealing a linear relationship between the output and the applied load while showing a linear temperature characteristic that suggests temperature compensation will be needed in use.

Keywords: force sensors; optical sensors; Fabry–Perot interferometer; surgical robotics

1. Introduction

Minimally invasive surgery (MIS) is a new surgical modality in which the surgeon inserts long instruments together with an endoscope inside the patient's body to reach a lesion. Because MIS greatly reduces the patients' physical burden and duration of hospital stay, it is beneficial both for patients and the medical economy. Although MIS has prominent benefits, it is widely known that MIS requires sophisticated manipulation skills from surgeons. Hence, surgical robots have been widely studied to provide assistance in MIS.

While force sensing and feedback in surgical robotic systems for MIS have a high potential for improving outcomes [1–4], there are no surgical robots capable of force feedback for soft tissue manipulation available on the current market. Force sensing would allow the surgeon to intuitively perceive the interaction force between the tissues and instruments, thus enabling the surgeon to properly adjust the force applied to the tissue. Optimizing the force on the tissues can minimize the damage caused by the manipulation [5]. In addition, the force interaction may provide further clinical information, functioning as a remote palpation that can be a key element of the procedure

(e.g., determining an organ’s hardness) [6,7]. Further, the development of fully or partly automated robotic surgical procedures based on machine learning has become a trend in the field of surgical robotics [8]. To pursue these highly integrated systems, along with vision and position data, additional information such as force interaction is required in most cases [9].

Despite these expected benefits, force sensing in surgical robots remains challenging for the following reasons. First, the force sensors must be implemented at the tip of instruments to avoid friction (which often occurs between the insertion port and the instrument or because of the internal structure of the instrument). To do so, the sensors must be small enough to be installed at the instrument tip. Because surgical instruments for MIS are generally 5 mm or smaller in diameter, such an implementation is challenging, because the internal mechanical elements (e.g., forceps drive shaft) should be intact but not influence the sensor output during motion. Second, the force sensor must be composed of biocompatible material and should be able to be sterilized. Last, the force sensor must be electrically safe for the patient and surgeon, but also tolerant of electric noise. This means that not only should there be no noise emitted from the sensor, the sensor should also be tolerant to the high levels of noise emitted from surgical energy devices, such as an electric knife.

In this study, we propose a new optical-based force sensor to fulfill the abovementioned requirements. For this purpose, we implemented the sensor as a modular sensor. Thus, similar to strain gauges, which are widely employed in the industry but do not meet the above restrictions, the sensor can be simply attached to a surgical robot or conventional instrument to provide the force information. In this paper, related work is described in the second section; the proposed concept and its implementation are described in the third section; experimental methods and results are described in the fourth section; and the discussion, conclusion, and future work are described in the last section.

2. Related Research

To pursue the study of force sensors in surgical devices, several sensing modalities have been introduced, namely, strain gauges, fiber-optics, and other modalities. The survey articles [10–12] introduce related research from a broad perspective. In this section, the related research on surgical applications is introduced according to sensing modality, as shown in Table 1.

Table 1. Force sensors in surgical devices.

Sensing Modality	Principle	References
Strain gauges	Electric resistance change	[13–18]
Fiber-optic	Light Intensity Modulation (LIM)	[19–21]
	Fiber-Bragg Grating (FBG)	[22–28]
	Fabry-Perot Interferometer (FPI)	[29–34]
	Other methods	[35,36]

2.1. Strain Gauges

Strain gauges are the most common force sensor in industry, and several attempts have been made to introduce them into the field of surgery [13–18]. The resistance of a strain gauge varies when the applied force and/or temperature change. It is commonly implemented by fabricating a thin structure in a mechanical structure to gain flexure and attaching the strain gauge in the proximity of this flexure. Zarrin et al. presented a flexure structure for forceps blades that allows two-degree-of-freedom force sensing by strain gauges [13]. Yu et al. presented a strain-gauge-attachable three-dimensional (3D) structure that can be implemented at the tip of a surgical instrument [14]. Matich et al. introduced a miniaturized surgical 3-D parallel mechanism that is implemented with a single axis force sensor at each end of the kinematic chain, thus enabling 3D force to be measured [15]. Seibold et al. presented a force-sensor integrated MIS robotic tool that allows 6-axis force sensing [16]. Hong et al. presented a flexure mechanism for forceps blades that can augment the strain at the flexure, thus improving the force-sensing capability [17]. Trejos studied the effect of autoclave sterilization on a strain gauge

attached to a surgical device [18]. The greatest challenge of the use of a strain gauge in surgical applications is that the sensor is not bio-compatible nor noise-tolerant in principle.

2.2. Fiber-Optic

There are three categories for fiber-optic force/pressure sensors: light intensity modulation (LIM) sensors, Fiber-Bragg gratings (FBG), and Fabry-Perot interferometers (FPI) [37]. The most advantageous feature of these fiber-optic sensors is that they are immune to electric noise.

2.2.1. Light Intensity Modulation (LIM)

When a modulator (e.g., mirror) rotates at the end of an optic-fiber, the reflected light intensity received through a fiber-optic varies substantially and is thus detectable after the light intensity is converted to a voltage. This principle can be used as a force sensor. Although the sensor structure can be simple and its measurement process is cost-effective, the sensor output of the light intensity tends to be influenced by the bending and deflection of the path of the optic fiber. Peirs et al. presented a surgical tool equipped with fiber-optic force sensors and tested it in an in-vivo experiment [19], Yip et al. presented a robust uniaxial force sensor using three optic fibers as a force sensing probe for cardiac surgery [20], and Noh et al. presented a three-axis fiber-optic body sensor for a flexible manipulator [21].

2.2.2. Fiber-Bragg Grating (FBG)

A diffraction grating formed by an ultra-violet laser in the optic fiber modulates a certain range of the spectrum of the reflected light [22]. The spectrum changes according to the applied deformation and/or temperature, and thus the FBG can be used as a force/temperature sensor. He et al. presented a 3-D force sensing surgical instrument for eye surgery with a diameter of less than 0.8 mm. In this device, three FBG optic fibers are attached along the long axis of the surgical instrument [23,24]. Gijbels et al. also presented a surgical instrument for eye surgery, implemented using FBG sensors [25]. Yokoyama et al. presented an FBG embedded irrigated radiofrequency ablation catheter [26]. Song et al. presented surgical robotic forceps with multiple degrees of freedom with embedded FBG sensors. The robotic forceps were specially designed to have flexure in the structure [27]. Arata et al. presented a backburn-shaped flexure design for force sensing using FBG [28].

2.2.3. Fabry-Perot Interferometer (FPI)

In an FPI, a micro electro mechanical system (MEMS) based transducer is attached at the end of an optic fiber that can convert the pressure applied on the transducer into a change in the spectrum of the reflected light. In general, an FPI achieves a higher accuracy or narrower spectrum measurement range, which drastically reduces the cost of the device. Totsu et al. presented an ultra-miniature fiber-optic pressure sensor [29]. In this study, we used the same sensor presented in [29]. The sensor's principle and implementation are described in the following section. Liu et al. presented surgical instruments for eye surgery implemented with FPI based force sensors [30] as an extension of [23,24]. Su et al. presented a miniature fiber-optic force sensor that is compatible with magnetic resonance imaging using FPI [31]. Beekmans et al. presented a force sensing needle that is integrated with a fiber-optic FPI on the tip [32]. Szczerska and Majchrowicz presented an FPI with thin ZnO layers deposited on on the end faces of the fiber-optic to form a cavity, and demonstrated its feasibility as a temperature sensor [33,34].

2.3. Other Methods

In contrast to the methods described above, Kim et al. presented a force sensor integrated in surgical forceps for MIS using capacitive transducers implemented at the jaws [35,36]. They reported

that the capacitance-to-digital converter chip implemented at the tip of the surgical instrument needs shielding because of its poor noise tolerance.

3. Method

In this section, the concept of the proposed sensor and its implementation are described.

3.1. Previously Developed Pressure Sensor

The proposed sensor employed an FPI-based pressure sensor previously proposed by one of the authors [29]. Figure 1 presents an overview of the previously developed sensor. The ultra-miniature fiber-optic pressure sensor (UMFOPS) had an FPI formed at the end of an optic fiber. A deformation of the diaphragm in the FPI induced by pressure varies the cavity length d , which can be detected by a spectrometer as a change in spectrum of the reflected light. This change is caused by the white light interferometry of the low-coherence light occurring in the FPI [38]. Therefore, d can be obtained by the following equation.

$$d = \frac{\lambda_1 \lambda_2}{2n(\lambda_2 - \lambda_1)}, \quad (1)$$

where n is the reflective index of the material of the sensor cavity and λ_1 and λ_2 are adjacent peaks in the reflection spectrum. UMFOPS is sterilizable, bio-compatible, miniaturized (125 μm in diameter), immune to electromagnetic noise, and has a low sensitivity to temperature change [29]. We selected the FPI sensor to be a key element of the proposed sensor, because, compared to an FBG, it has a lower temperature sensitivity and a narrower wavelength range that must be monitored. Because the range of measurable wavelength predominantly affects the cost of the spectrometer thus the device, the narrower wavelength range is an advantage for further applications.

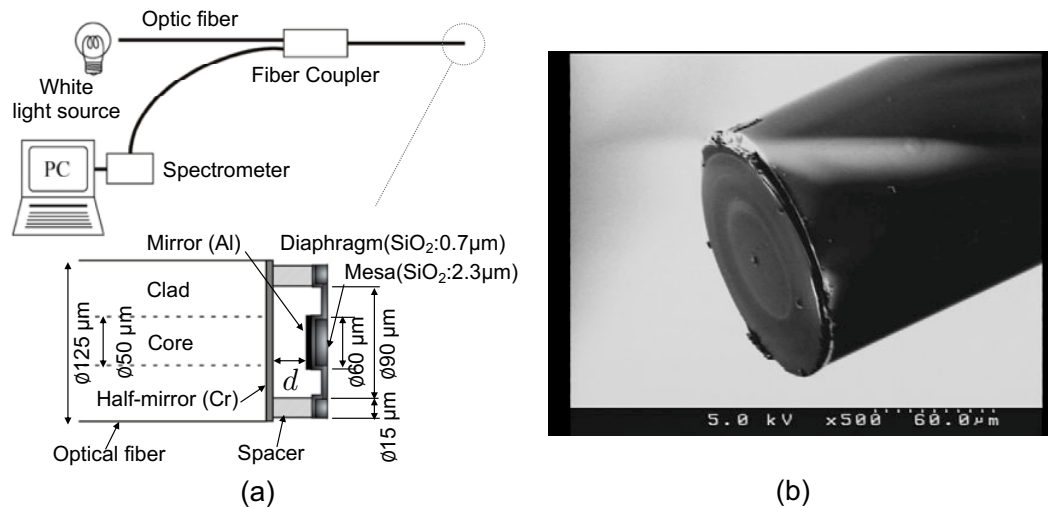


Figure 1. Previously developed Fabry–Perot interferometer (FPI)-based ultra-miniature fiber-optic pressure sensor (UMFOPS) pressure sensor [29]: (a) system overview and (b) close-up image of the sensor.

3.2. Proposed Force Sensor

The proposed sensor is an extension of the previously proposed pressure sensor into a force sensor. The design was made to be modular so that the sensor can be applied in different medical instruments, including conventional surgical tools. Figure 2 illustrates the structure of the proposed sensor. It consists of sensor housings A and B (SUS304), a carbide pin (Unitech, Kanagawa, Japan), and a UMFOPS. The UMFOPS and carbide pin were adhered in the slot fabricated on sensor housing B using low-temperature sealing glass. When adhered, the two elements were preloaded against

each other enable both compression and elongation forces to be measured. After the adhesion, the components were covered by sensor housing A. The proposed sensor structure enabled deformation along the long axis; this deformation is detectable by the UMFOPS. The structure is sterilizable and bio-compatible. Because no electric elements exist in the structure, the sensor is inherently immune to electromagnetic noise. Moreover, because the sensor structure is miniaturized and modularized, the sensor can be easily integrated into various surgical devices.

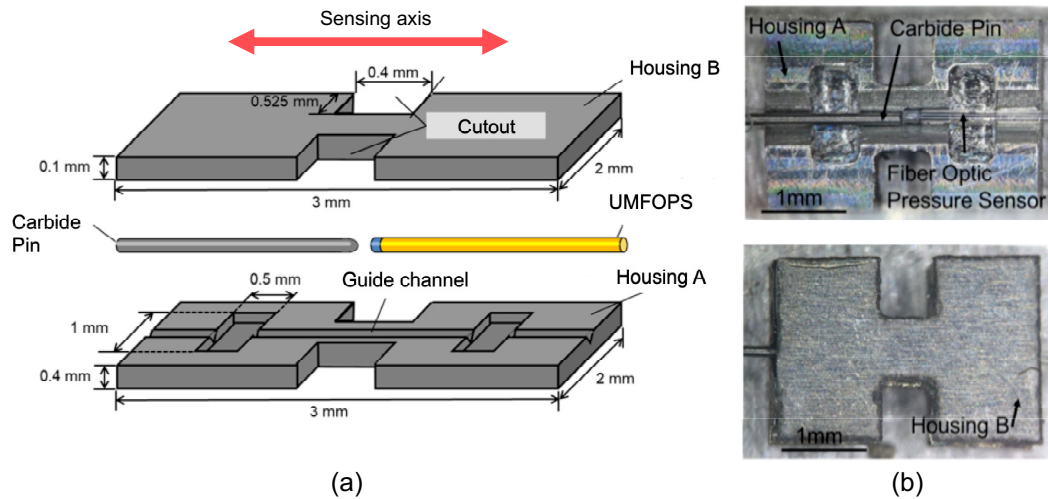


Figure 2. Structure of the proposed force sensor: (a) overview and (b) images of the developed sensor.

3.3. Implementation

The proposed sensor was implemented using the following processes. First, sensor housings A and B were fabricated from stainless steel (SUS304) by high-precision metal cutting. A guide channel with a V-notch was fabricated in the center of housing A, to precisely align the carbide pin and the UMFOPS. The cutout from both sides of housing A were fabricated to increase the sensitivity. The carbide pin was custom-ordered with a diameter of 120 μm (WH20, Unitech, Kanagawa, Japan). The assembly process was performed manually, as shown in Figure 3. The most important part of this process is the heating and cooling (shown in Figure 3 (2) and (3)). The heating process rigidly fixes the carbide pin and UMFOPS together with low-temperature sealing glass. This process is required not only for the low-temperature sealing glass to adhere, but also so that the cooled sensor structure compresses the carbide pin and UMFOPS together, enabling both pushing and pulling forces to be measured. All procedures were conducted manually using a microscope and the positioning stage shown in Figure 4.

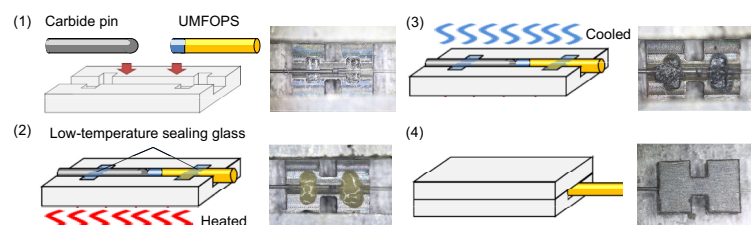


Figure 3. Sensor assembly: (1) The carbide pin and UMFOPS are aligned in the channel in sensor housing A so that their tips are in contact. (2) The buffers are filled with low-temperature sealing glass and heated to 300 $^{\circ}\text{C}$. (3) The sensor is cooled to 25 $^{\circ}\text{C}$. Pre-compression is achieved by the thermal deformation of the sensor structure during cooling. (4) The sensor is covered and sealed by sensor housing B.

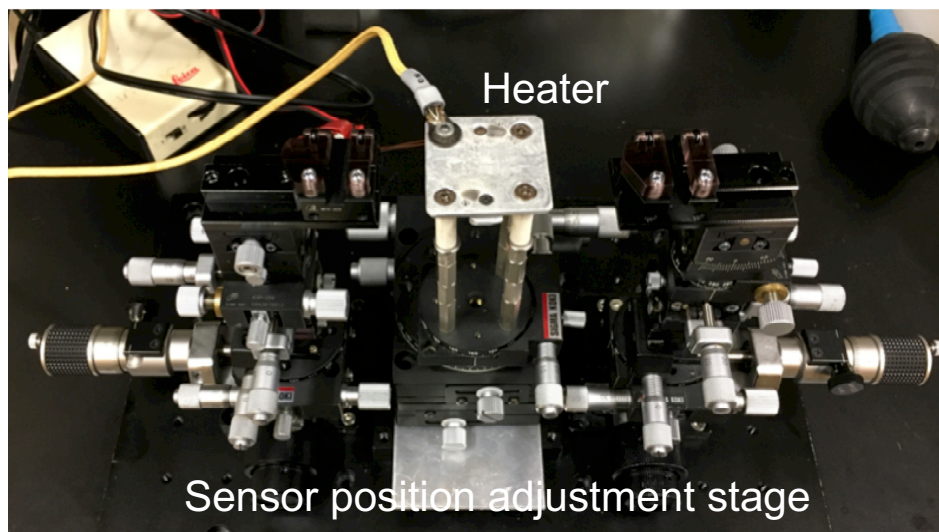


Figure 4. Positioning stage with an integrated temperature-controlled heater for sensor assembly.

4. Evaluation

To evaluate the developed sensor, load and temperature characteristic tests were conducted.

4.1. Experimental Setup

The developed sensor was attached to a fiber coupler and white light source (LED-VRwhite-15-CT, FiberLabs), while the reflective light was monitored by a spectrometer (USB4000, Ocean Optics, USA). The sensor output was monitored by a PC connected to the spectrometer via USB.

4.2. Load Test

To test the feasibility of the sensor as a force sensor, the developed sensor was attached to a test piece with a V-notch in the middle, as shown in Figure 5. Note that the test piece was fabricated considering applications in surgery (e.g., putting a force sensor on conventional surgical forceps). The load was applied by a motorized precision stage (OSMS26, Sigmakoki, Japan) with a force gauge (ZTA-50N, IMADA, Japan). In the experiment, ± 25 N tension and compression were applied using the experimental setup shown in Figure 5.

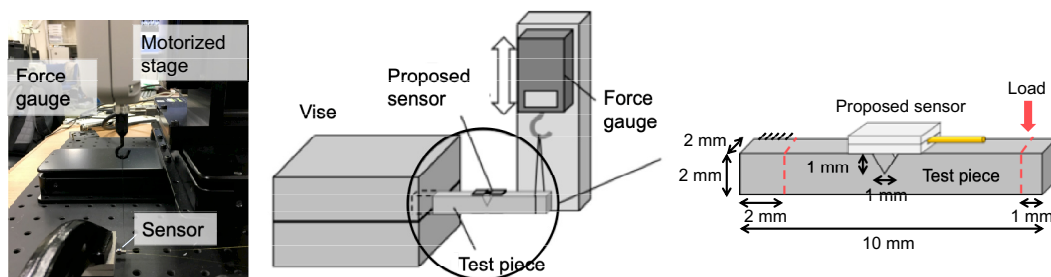


Figure 5. Load test setup. The developed sensor was attached over the V-notch of a test piece. Force was applied at the end of test piece while the other end was fixed by a vise.

The measurement was conducted three times, and each result showed the same tendency. A representative experimental result is shown in Figure 6. A linear output characteristic of the proposed sensor is suggested by the result with a correlation coefficient of 0.998. The resolution of the sensor in

this experimental setup was computed to be 119 mN with a range of ± 25 N, while the sensitivity was found to be 2.52 nm/N.

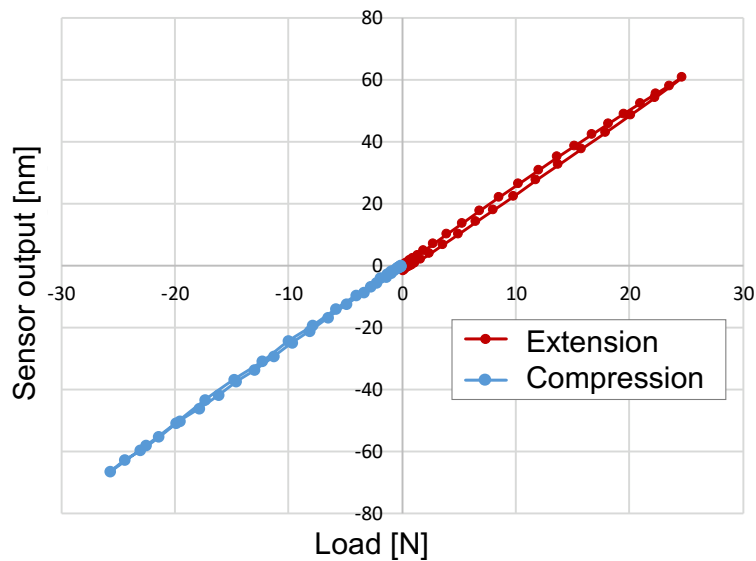


Figure 6. Load test result. A linear output characteristic is suggested with a correlation coefficient of 0.998.

4.3. Temperature Characteristic Test

The temperature characteristic of the sensor was tested for two different cases: (1) the sensor module only and (2) the sensor attached to the test piece described in the load test. In both cases, the sensor was placed in a temperature chamber (SU-641, Espec, Japan), and the temperature was first increased from 5 to 45 °C and then decreased to 5 °C again.

The experimental results (Figure 7 show that the sensor output linearly increases when the temperature changes. This measurement was also conducted three times, and the results showed the same tendency. A representative experimental result is shown in Figure 7. In the measurement, no hysteresis was observed. The correlation coefficient was found to be 0.999 for both cases. As suggested in [29], UMFOPS does have a temperature-dependent characteristic. Therefore, the temperature characteristic observed in this experiment may be caused by the sensor structure. The sensitivity was found to be 2.36 nm/°C for the sensor alone and 2.61 nm/°C for the sensor with the test piece. The characteristics of the developed sensor are summarized Table 2.

Table 2. Characteristics of proposed fiber-optic force sensor.

Characteristic	Value
Dimension	$3 \times 2 \times 0.5$ mm
Force range	± 25 N
Range of wavelength shift	−66.7 to 60.8 nm
Correlation coefficient of the output	0.999
Resolution	0.235 %FS
Temperature characteristic	2.36 nm/°C or 0.94 nm/N

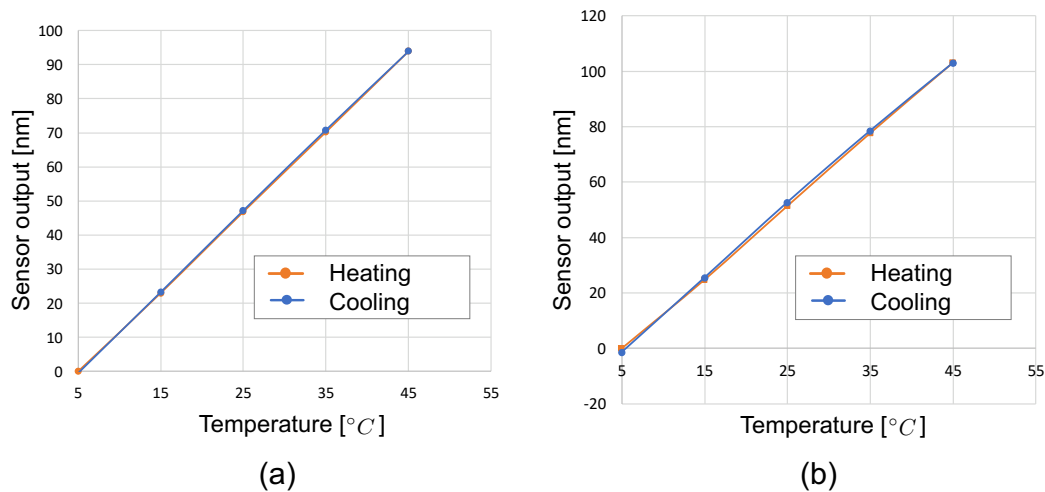


Figure 7. Temperature test results: (a) results for only the sensor module and (b) results for the sensor attached to the test piece shown in Figure 5. Both results suggest a linear temperature characteristic.

5. Discussion and Conclusion

In this paper, we proposed a new design for a fiber-optic force sensor that can be used for surgical devices. The proposed sensor is a modification of an FPI sensor previously proposed by one of the co-authors [29]. The proposed sensor has a linear output characteristic and is bio-compatible and sterilizable. The most advantageous feature of the proposed sensor is its modularity. It can be attached to conventional surgical devices like a strain gauge to provide force information at the tip. In the evaluation, a temperature characteristic was observed due to the sensor structure. The overall results show the promising feasibility of its use in surgical applications.

One of the greatest challenges for the mass production of this sensor is that manual assembly procedures are prone to human error and thus could be a source of inaccuracy. A calibration procedure would be necessary for each device in the current assembly procedure. Further improvement of this process will be necessary for future mass production.

The sensitivity was found to be 2.36–2.61 nm/°C. This could be improved by using a less rigid material for the sensor housing. In this study, we used stainless steel because of the ease of production and its linear characteristic between deformation and load. However, because we have a large margin of measurable wavelength (e.g., 200–1100 nm with the current setup), a softer material for the sensor structure would drastically improve sensitivity. A spectrometer with a higher resolution would also improve the sensitivity.

As was suggested by the experimental results, the temperature characteristic is mainly caused by the sensor structure fabricated from stainless steel. A less thermally sensitive material would drastically reduce the effects of temperature; however, this characteristic will probably remain to some degree and be difficult to remove. Because the sensor has a linear relationship with temperature change, it is possible that the sensor can be used with a temperature compensator (e.g., a Wheatstone bridge), which is commonly used for strain gauges with multiple sensor elements. This would require the applications to implement multiple sensors; however, this would be useful for some applications that require simultaneous force and temperature measurements.

In this paper, the sensor was tested in a static condition, and dynamic conditions such as time-response were not tested. However, the principle of FPI allows for real-time measurement [29], and our preliminary tests show that it seems feasible.

The technical contribution of this paper is the proposal of a force sensor structure based on an FPI fiber-optic pressure sensor. The proposed structure realizes a force sensor that is bio-compatible,

sterilizable, noise-tolerant, and most importantly, modular, which allows the user to measure the force applied on a conventional surgical device by attaching the proposed sensor.

The proposed sensor has been specifically designed for surgical application, enabling the structure to be bio-compatible, sterilizable, and tolerant to noise within the miniaturized size. An example application would be to put the proposed sensor into the jaws of surgical forceps to measure the force applied to the organs. Because the sensor is bio-compatible, sterilizable, and tolerant to noise within the miniaturized size, it can be placed close to lesions, where a small interaction force between the instruments and the organ can be measured without additional disturbance (e.g., friction in the mechanism of the instruments). Further, we are currently working on the improvements discussed in this section and further plan to implement the sensor in a surgical robot [39–41].

6. Patents

A patent was submitted based on the technology shown in this paper (Application No. 2018-081708, submitted on 20 April 2018).

Author Contributions: conceptualization, J.A., T.M., Y.H., K.H., and M.M.; methodology, J.A., T.N. (Tatsuya Nitta), T.N. (Toshiki Nakatsuka), T.M., and Y.H.; software, T.K.; validation, T.N. (Tatsuya Nitta), T.N. (Toshiki Nakatsuka), and T.M.; writing—review and editing, J.A.; visualization, J.A. and T.N. (Tatsuya Nitta); supervision, J.A.; project administration, M.M.; funding acquisition, K.H. and J.A.

Funding: Part of this work was supported by the ImPACT Program of the Council for Science, Technology, and Innovation (Cabinet Office, Government of Japan), and JSPS KAKENHI Grant Number JP18959353.

Conflicts of Interest: The authors declare no conflict of interest.

References

1. Tholey, G.; Desai, J.P.; Castellanos, A.E. Force feedback plays a significant role in minimally invasive surgery results and analysis. *Ann. Surg.* **2005**, *241*, 102–109. [[PubMed](#)]
2. Taylor, R.H.; Menciassi, A.; Fichtinger, G.; Dario, P. Medical robotics and computer-integrated surgery. In *Springer Handbook of Robotics*; Springer: Berlin, Germany, 2008; Chapter 52, pp. 1199–1222.
3. Okamura, A.M. Methods for haptic feedback in teleoperated robot-assisted surgery. *Ind. Rob.* **2004**, *31*, 499–508. [[CrossRef](#)] [[PubMed](#)]
4. Haidegger, T.; Benyó, B.; Kovács, L.; Benyó, Z. Force sensing and force control for surgical robots. In Proceedings of the 7th IFAC Symposium on Modelling and Control in Biomedical Systems, Aalborg, Denmark, 12–14 August 2009; pp. 401–406.
5. Braun, E.U.; Mayer, H.; Knoll, A.; Lange, R.; Bauernschmitt, R. The must-have in robotic heart surgery: Haptic feedback. In *Medical Robotics*; Intech Open: London, UK, 2008; Chapter 2, pp. 9–20.
6. Howe, R.D.; Peine, W.J.; Kontarinis, D.A.; Son J.S. Remote palpation technology. *IEEE Eng. Med. Biol. Mag.* **1995**, *14*, 318–323. [[CrossRef](#)]
7. Mahvash, M.; Gwilliam, J.; Agarwal, R.; Vagvolgyi, B.; Su, L.M.; Yuh, D.D.; Okamura, A.M. Force-feedback surgical teleoperator: Controller design and palpation experiments. In Proceedings of the 2008 Symposium on Haptic Interfaces for Virtual Environment and Teleoperator Systems, Reno, NE, USA, 13–14 March 2008; pp. 465–471.
8. Yang, G.Z.; Bellingham, J.; Dupont, P.E.; Fischer, P.; Floridi, L.; Full, R.; Jacobstein, N.; Kumar, V.; McNutt, M.; Merrifield, R.; et al. The grand challenges of Science Robotics. *Sci. Robot.* **2018**, *3*, eaar7650. [[CrossRef](#)]
9. Shademan, A.; Decker, R.S.; Opfermann, J.D.; Leonard, S.; Krieger, A.; Kim, P.C.W. Supervised autonomous robotic soft tissue surgery. *Sci. Transl. Med.* **2016**, *8*, 337ra64. [[CrossRef](#)] [[PubMed](#)]
10. Althoefer, K.; Liu, H.; Puangmali, P.; Zbyszewski, D.; Noonan, D.; Seneviratne, L.D. Force sensing in medical robotics, In *Mechatronics in Action: Case Studies in Mechatronics—Applications and Education*; Springer: Berlin, Germany, 2019; Chapter 1.
11. Trejos, A.L.; Patel, R.V.; Naish, M.D. Force sensing and its application in minimally invasive surgery and therapy: A survey. *Proc. Inst. Mech. Eng. Part C J. Mech. Eng. Sci.* **2010**, *224*, 1435–1454. [[CrossRef](#)]

12. Puangmali, P.; Althoefer, K.; Seneviratne, L.D. State-of-the-art in force and tactile sensing for minimally invasive surgery. *IEEE Sens. J.* **2008**, *8*, 371–381. [[CrossRef](#)]
13. Zarrin, P.S.; Escoto, A.; Xu, R.; Patel, R.V.; Naish, M.D.; Trejos, A.L. Development of a 2-DOF sensorized surgical grasper for grasping and axial force measurements. *IEEE Sens. J.* **2018**, *18*, 2816–2826. [[CrossRef](#)]
14. Yu, L.; Yan, Y.; Yu, X.; Xia, Y. Design and realization of forceps with 3-D force sensing capability for robot-assisted surgical system. *IEEE Sens. J.* **2018**, *18*, 8924–8832. [[CrossRef](#)]
15. Matich, S.; Neupert, C.; Kirschniak, A.; Schlaak, H.F.; Pott, P. 3-D force measurement using single axis force sensors in a new single port parallel kinematics surgical manipulator. In Proceedings of the 2016 IEEE/RSJ International Conference on Intelligent Robots and Systems (IROS), Daejeon, Korea, 9–14 October 2016; pp. 3665–3670.
16. Seibold, U.; Kübler, B.; Hirzinger, G. Prototype of instrument for minimally invasive surgery with 6-axis force sensing capability. In Proceedings of the 2005 IEEE International Conference on Robotics and Automation, Barcelona, Spain, 18–22 April 2005; pp. 496–501.
17. Hong, M.B.; Jo, Y.H. Design and evaluation of 2-DOF compliant forceps with force-sensing capability for minimally invasive robot surgery. *IEEE Trans. Robot.* **2012**, *28*, 932–941. [[CrossRef](#)]
18. Trejos, A.L.; Escoto, A. Design and evaluation of a sterilizable force sensing instrument for minimally invasive surgery. *IEEE Sens. J.* **2017**, *17*, 3983–3993. [[CrossRef](#)]
19. Peirs, J.; Clijnen, J.; Reynaerts, D.; Brussel, H.V.; Herijgers, P.; Corteville, B.; Boone, S. A micro optical force sensor for force feedback during minimally invasive robotic surgery. *Sens. Actuators A* **2004**, *115*, 447–455. [[CrossRef](#)]
20. Yip, M.C.; Yuen, S.G.; Howe, R.D. A robust uniaxial force sensor for minimally invasive surgery. *IEEE Trans. Biomed. Eng.* **2010**, *57*, 1008–1011. [[CrossRef](#)] [[PubMed](#)]
21. Noh, Y.; Sareh, S.; Würdemann, H.; Liu, H.; Back, J.; Housden, J.; Rhode, K.; Althoefer, K. Three-axis fiber-optic body force sensor for flexible manipulators. *IEEE Sens. J.* **2016**, *16*, 1641–1651. [[CrossRef](#)]
22. Hill, K.O.; Meltz, G. Fiber bragg grating technology fundamentals and overview. *J. Lightwave Technol.* **1997**, *15*, 1263–1276. [[CrossRef](#)]
23. He, X.; Handa, J.; Gehlbach, P.; Taylor, R.; Iordachita, I. A submillimetric 3-DOF force sensing instrument with integrated fiber bragg grating for retinal microsurgery. *IEEE Trans. Biomed. Eng.* **2014**, *61*, 522–534. [[PubMed](#)]
24. Gonenc, B.; Chae, J.; Gehlbach, P.; Taylor, R.H.; Iordachita, I. Towards robot-assisted retinal vein cannulation: A motorized force-sensing microneedle integrated with a handheld micromanipulator. *Sensors* **2017**, *17*, E2195. [[CrossRef](#)] [[PubMed](#)]
25. Gijbels, A.; Vander Poorten, E.B.; Stalmans, P.; Reynaerts, D. Development and experimental validation of a force sensing needle for robotically assisted retinal vein cannulations. In Proceedings of the 2015 IEEE International Conference on Robotics and Automation (ICRA), Seattle, WA, USA, 2015; pp. 2270–2276.
26. Yokoyama, K.; Nakagawa, H.; Shah, D.C.; Lambert, H.; Leo, G.; Aeby, N.; Ikeda, A.; Pitha, J.V.; Sharma, T.; Lazzara, R.; et al. Novel contact force sensor incorporated in irrigated radiofrequency ablation catheter predicts lesion size and incidence of steam pop and thrombus. *Circ. Arrhythm. Electrophysiol.* **2008**, *1*, 354–362. [[CrossRef](#)] [[PubMed](#)]
27. Song, H.; Kim, K.; Lee, J. Development of optical fiber Bragg grating force-reflection sensor system of medical application for safe minimally invasive robotic surgery. *Rev. Sci. Instrum.* **2011**, *82*, 074301. [[CrossRef](#)] [[PubMed](#)]
28. Arata, J.; Terakawa, S.; Fujimoto, H. Fiber optic force sensor for medical applications within a backbone-shape structure. *Proc. CIRP*, **2013**, *5*, 66–69. [[CrossRef](#)]
29. Totsu, K.; Haga, Y.; Esashi, M. Ultra-miniature fiber-optic pressure sensor using white light interferometry. *J. Micromech. Microeng.* **2004**, *15*, 71–75. [[CrossRef](#)]
30. Liu, X.; Iordachita, I.; He, X.; Taylor, R.H.; Kang, J.U. Miniature fiber-optic force sensor based on low-coherence Fabry-Pérot interferometry for vitreoretinal microsurgery. *Biomed. Opt. Express* **2012**, *3*, 1062–1076. [[CrossRef](#)] [[PubMed](#)]
31. Su, H.; Zervas, M.; Furlong, C.; Fischer, G.S. A miniature MRI-compatible fiber-optic force sensor utilizing fabry-perot interferometer MEMS and nanotechnology. In *Proceedings of the 2011 Annual Conference on Experimental and Applied Mechanics*; Springer: Berlin, Germany, 2011; pp. 131–136.

32. Beekmans, S.; Lembrechts, T.; van den Dobbelsteen, J.; van Gerwen, D. Fiber-optic fabry-pérot interferometers for axial force sensing on the tip of a needle. *Sensors* **2017**, *17*, 38. [[CrossRef](#)] [[PubMed](#)]
33. Jedrzejewska-Szczerska, M.; Wierzba, P.; Chaaya, A.A.; Bechelany, M.; Miele, P.; Viter, R.; Mazikowski, A.; Karpienko, K.; Wrobel, M. ALD thin ZnO layer as an active medium in a fiber-optic Fabry-Perot interferometer. *Sens. Actuators A Phys.* **2016**, *221*, 88–94. [[CrossRef](#)]
34. Majchrowicz, D.; Hirsch, M.; Wierzba, P.; Bechelany, M.; Viter, R.; Szczerska M.J. Application of thin ZnO ALD layers in fiber-optic fabry-Pérot sensing interferometers. *Sensors* **2015**, *16*, 416. [[CrossRef](#)] [[PubMed](#)]
35. Kim, U.; Lee, D.; Yoon, W.J.; Hannaford, B.; Choi, H.R. Force sensor integrated surgical forceps for minimally invasive robotic surgery. *IEEE Trans. Robot.* **2015**, *31*, 1214–1224. [[CrossRef](#)]
36. Kim, U.; Kim, Y.B.; So, J.; Seok, D.; Choi, H.R. Sensorized surgical forceps for robotic-assisted minimally invasive surgery. *IEEE Trans. Ind. Electron.* **2018**, *65*, 9604–9613. [[CrossRef](#)]
37. Polygerinos, P.; Zbyszewski, D.; Schaeffter, T.; Razavi, R.; Seneviratne, L.D.; Althoefer, K. MRI-compatible fiber-optic force sensors for catheterization procedures. *IEEE Sens. J.* **2010**, *10*, 1598–1608. [[CrossRef](#)]
38. Belleville, C.; Duplain, G. White-light interferometric multimode fiber-optic strain sensor. *Opt. Lett.* **1993**, *18*, 78–80. [[CrossRef](#)]
39. Arata, J.; Fujisawa, Y.; Nakadate, R.; Harada, K.; Mitsuishi, M.; Kiguchi, K.; Hashizume, M. Synthetic elastic mechanism for miniaturized neurosurgical robotic forceps. *Int. J. CARS* **2018**, *12* (Suppl. 1), S44–S45.
40. Arata, J.; Fujisawa, Y.; Nakadate, R.; Kiguchi, K.; Harada, K.; Mitsuishi, M.; Hashizume, M. Compliant four degree-of-freedom manipulator with locally deformable elastic elements for minimally invasive surgery. In Proceedings of the International Conference on Robotics and Automation, Montreal, Canada, 20–24 May 2019; pp. 2663–2669.
41. Arata, J.; Bandara, S.V.; Kajihara, W.; Nakadate, R.; Harada, K.; Mitsuishi, M.; Hashizume, M. 2mm surgical manipulator with four degrees-of-freedom for transnasal endoscopy comprising elastic mechanical elements. *Int. J. CARS* **2019**, *14* (Suppl. 1), S48–S49.



© 2019 by the authors. Licensee MDPI, Basel, Switzerland. This article is an open access article distributed under the terms and conditions of the Creative Commons Attribution (CC BY) license (<http://creativecommons.org/licenses/by/4.0/>).